Journal of the European Optical Society - Rapid Publications 5, 10002 (2010) www.jeos.org

Electro-optically induced absorption in α-Si:H/α-SiCN waveguiding multistacks

Sandro Rao
sandro.rao@unirc.it
Department of Information Science, Mathematics, Electronics and Transportations (DIMET) "Mediterranea" University, Via Graziella Località Feo di Vito, Reggio Calabria, 89060, Italy

Francesco G. Della Corte
Department of Information Science, Mathematics, Electronics and Transportations (DIMET) "Mediterranea" University, Via Graziella Località Feo di Vito, Reggio Calabria, 89060, Italy

Caterina Summonte
Institute for Microelectronics and Microsystems, Consiglio Nazionale delle Ricerche - Unit of Bologna, Via Gobetti 101, Bologna, 40129, Italy.

Electro optical absorption in hydrogenated amorphous silicon (α-Si:H)-amorphous silicon carbonitride (α-SiC$_x$N$_y$) multilayers have been studied in three different planar multistacks waveguides. The waveguides were realized by plasma enhanced chemical vapour deposition (PECVD), a technology compatible with the standard microelectronic processes. Light absorption is induced at $\lambda = 1.55$ μm through the application of an electric field which induces free carrier accumulation across the multiple insulator/semiconductor device structure. The experimental performances have been compared to those obtained through calculations using combined two-dimensional (2-D) optical and electrical simulations. [DOI: 10.2971/jeos.2010.10002]

Keywords: amorphous silicon, integrated optics, silicon opto-electronics, electro-optics, free carrier absorption, waveguides

1 INTRODUCTION

Hydrogenated amorphous silicon (α-Si:H) shows interesting features which make it attractive for lightwave communication purposes; it is transparent in the infrared [1], exhibits refractive index tunability by acting on the process parameters, and has a very good technological compatibility with microelectronics, due in particular to the low thermal budget involved in its deposition and structuring, which can take place at $T < 250°$C, for example, at the end of the CMOS process flow. Many applications have been already proposed for this material in the optical communication area for the detection of photons [2], and for lightwave guiding [3, 4].

Thermo-optical and all-optical effects have also been exploited in α-Si:H to demonstrate modulation or switching action in planar devices for integrated photonics [3, 5]. Electro-optical effects, in contrast, have been rarely considered in this material due to the weak incidence of electric field on the refractive index [6], on one side, and the difficulty of reaching a significant carrier injection across p-n junctions in amorphous semiconductors, on the other side.

In this paper we report results on a field effect induced light modulation at $\lambda = 1.55$ μm in α-Si:H/α-SiCN multi-stack planar waveguiding structures deposited by PECVD on a c-Si substrate. The modulation mechanism has been modelled as a free carrier effect on the imaginary part of the refractive index. In particular, the absorption is enhanced by carrier accumulation at the intermediate semiconductor/insulator interfaces. The carrier profile under bias was estimated by means of electrical simulations and used for optical simulations. The results are found to be in agreement with the experimental data.

2 DESIGN AND FABRICATION

We designed and fabricated three different waveguides. The first waveguide (see Figure 1(a)) consists of the stack of three bi-layers each composed of a 1 μm-thick α-Si:H layer and a 30 nm-thick α-SiCN layer, deposited on a <100> heavily doped Silicon substrate. The substrate and the stack are separated by a 0.39 μm-thick Si_3N_4low refractive index cladding layer. The second waveguide (see Figure 1(b)) differs from the first one in that it is made of six stacked bi-layers each composed of a 0.5 μm-thick α-Si:H layer and a 40 nm-thick α-SiCN layer. The third structure differs from the second one in that the α-Si:H layers are 0.2 μm-thick. A 80 nm-thick transparent conductive Indium Tin Oxide (ITO) thin film forms the top contact, while the bottom contact is the Si substrate itself.

In all cases, due to the steep change in the refractive indices of a-Si:H and Si_3N_4, $\Delta n \approx 2$, a strong vertical confinement is achieved. The fabrication of the three bi-layer waveguides begins with a surface cleaning treatment, using H_2SO_4+H_2O_2 and HF solutions on the n-type highly doped c-Si substrate ($\rho = 0.001$ $\Omega \cdot$ cm). The substrate is then loaded into the four-chamber RF (13.56 MHz) system. First, the Si_3N_4 cladding layer is deposited from the plasma-assisted decomposition of SiH_4 and NH_3, at a RF power $P_{RF} = 4$ W. Subsequently, the first α-Si:H layer is deposited in SiH_4 atmosphere, followed by the deposition of the α-SiCN layer from a gaseous mixture of SiH_4, NH_3 and CH_4. The forth/fifth and sixth/seventh deposition steps are made under the same conditions as the second/third ones. Temperature is 220°C for all steps. The 80 nm-thick top ITO film is deposited by magnetron sputtering. The

Received December 01, 2009; published January 17, 2010 ISSN 1990-2573

Material	T (°C)	Rate (As^{-1})	Process Gas (sccm)		n	α (cm^{-1})	σ (Scm^{-1})
Si_3N_4	220	2.5	SiH_4 NH_3	1.5 68	1.77 ± 0.02	10 ± 5	$< 10^{-16}$
α-Si:H	220	1.5	SiH_4	20	3.58 ± 0.02	1 ± 0.5	2.6×10^{-9}
α-SiCN	220	1.62	SiH_4 NH_3 CH_4	8 24 8	2.03 ± 0.02	3 ± 1.5	5.2×10^{-16}

TABLE 1 PECVD process parameters: substrate temperature, deposition rate. Refractive index n and absorption coefficient α are measured at 1.55 μm. Conductivity measurements were performed using a computer controlled parametric characterization system based on an automatic probing station.

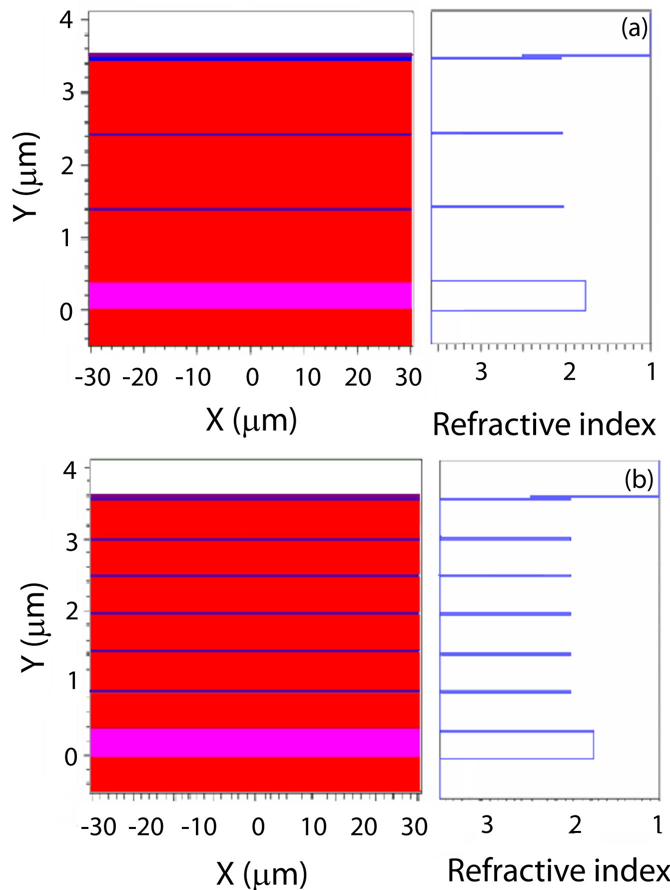

FIG. 1 Schematic cross sections of the realised planar waveguides and corresponding refractive index profiles. The crystalline silicon substrate is 300 μm thick.

fabrication of the six bi-layer waveguides followed the same procedure. The fundamental process parameters and material characteristics at $\lambda = 1.55$ μm are listed in Table 1).

In our devices the thin α-SiCN highly insulating layers ($\sigma = 5.2 \times 10^{-16}$ Scm^{-1}) break the conduction between the α-Si:H films so that the device electrically behaves as a series of capacitors. The ternary alloy SiC_xN_y has in fact good insulating properties and forms good interfaces with amorphous silicon. For this reason it has been exploited as the dielectric layer in α-Si:H thin film transistors (TFTs) in place of the traditional SiN_x gate insulator [7].

The application of a voltage across the stack therefore produces an accumulation of electrons and holes respectively at the opposite sides of each insulating film, and therefore at intermediate depths across the waveguide. This approach has been theoretically proven to enhance the effects induced by free carriers on the optical propagation characteristics of c-Si waveguides [8].

3 RESULTS

The principle used to modulate the light signal is the variation of the free carrier concentration at the multiple α-Si:H/α-SiCN interfaces. The Si refractive index and absorption coefficient depend on the free carrier concentration by the dispersion relation [9] that can be derived, to a first order approximation, from the classical Drude model,

$$\Delta n = -\frac{e^2\lambda^2}{8\pi^2c^2\epsilon_0 n}\left(\frac{\Delta N_e}{m_e}+\frac{\Delta N_h}{m_h}\right)$$
$$\Delta\alpha = \frac{e^2\lambda^2}{4\pi^2c^2\epsilon_0 n}\left(\frac{\Delta N_e}{m_e^2\mu_e}+\frac{\Delta N_h}{m_h^2\mu_h}\right) \quad (1)$$

where Δn and $\Delta\alpha$ are the variations of the real part of the refractive index, n, and of the absorption coefficient, α, respectively due to the free carrier concentration change, e is the electron charge, ϵ is the permittivity in free space, n is the refractive index of intrinsic Si, μ is the free carrier mobility, m is the effective mass, ΔN is the free carrier concentration variation, and λ is the wavelength. The subscripts e and h refer to electrons and holes, respectively.

The effect of the introduction of more α-SiCN regions is a distribution of the excess free carriers across the device section, and consequently an enhancement of the modulation efficiency. The carrier distributions under bias were first determined in the structure by performing electrical simulations with a finite element CAD code specifically designed for the simulation of solid-state devices including amorphous semiconductor regions, *ATLAS-TFT*. We calculated the electrons and holes profiles at each α-Si:H/α-SiCN interface. We obtained a carrier concentration change, close to the interface, of $\sim 10^{18}$ cm^{-3} when a bias of 30 V is applied across the three bi-layer device. Figure 2 reports the geometrical details (see Figure 2(b)) of one of the three insulator-silicon-insulator structures forming the device, and the calculated electron concentration depth profile (see Figure 2(a)).

In our experiments the probe beam was a 15 mW laser diode radiation ($\lambda = 1.55$ μm), coupled to the waveguide core via an 8 μm core monomode fiber. The transmitted light was collected at the chip output by a multimode fiber and detected by an InGaAs photodiode. With this setup, the propagation losses were measured by the cut-back technique. Several sam-

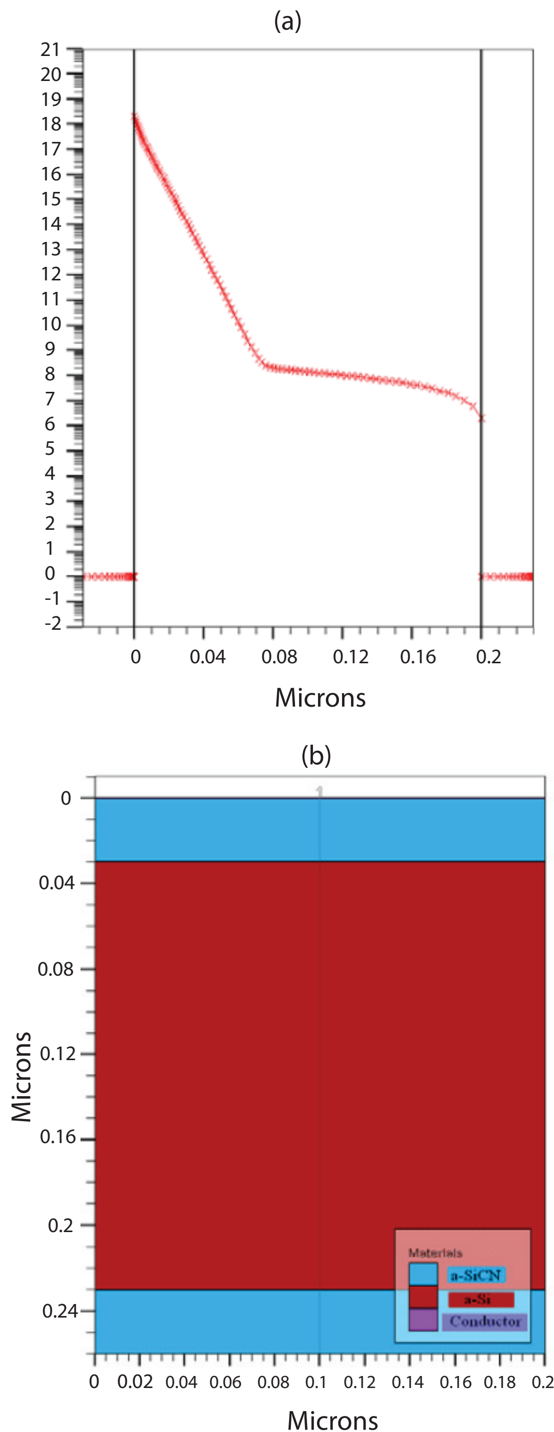

FIG. 2 Estimated electron concentrations/log(cm^{-3}) (a) along a vertical section from the centre of the device (b). The applied voltage is 30 V.

ples with lengths in the range 0.5 cm to 1.5 cm were cut from the substrate by cleavage. Sample facets did not receive polishing treatment. We calculated a loss coefficient of 2.25 ± 0.03 cm^{-1} for the three-layers waveguide, 2.77 ± 0.09 cm^{-1} for the six-layers waveguide (0.5 μm-thick α-Si:H layer) and 2.26 cm^{-1} for the six-layers waveguide (0.2 μm-thick α-Si:H layer) which are in the ranges estimated by simulations.

The propagation characteristics of the waveguides were studied by means of a numerical electromagnetic-wave solver based on the Beam Propagation Method (BPM) [10].

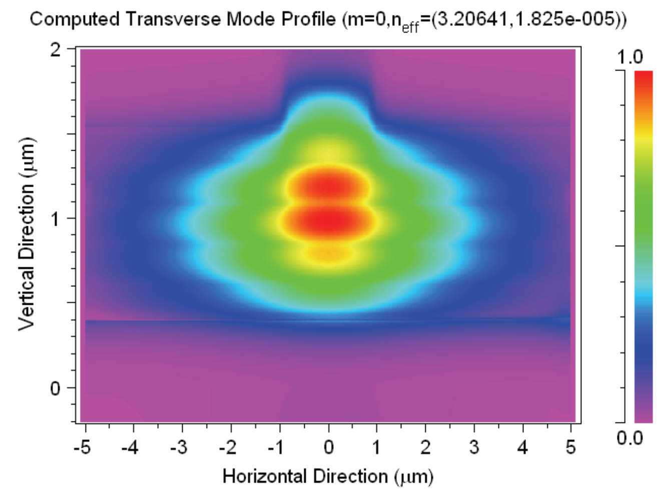

FIG. 3 TE fundamental optical mode-field profile of the thin six bi-layer waveguide.

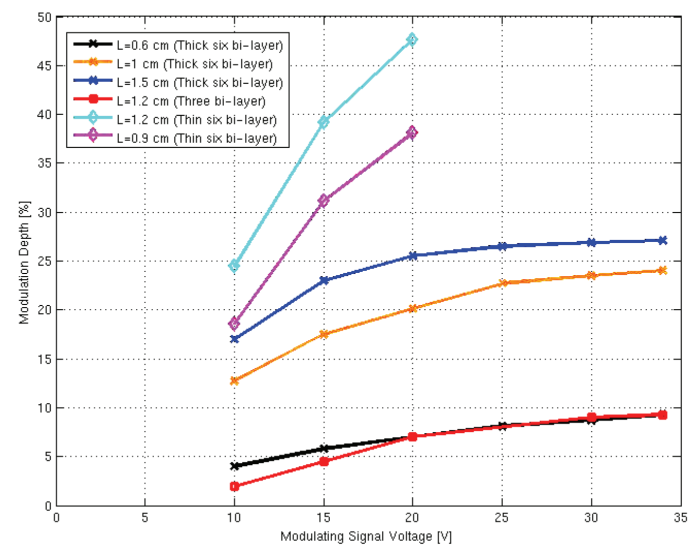

FIG. 4 Dependence of $M_{\%}$ on the modulating signal amplitude for three and six bi-layer samples.

The simulator predicts, for the six-layers waveguide (0.2 μm-thick α-Si:H layer), that single mode operation is obtained once a 2 μm wide rib is defined by etching 0.35 μm the top layers. This geometry satisfies the single mode condition proposed by Soref *et al.* [11].

Figure 3 shows the fundamental TE_0 mode, well confined under rib region, characterized by propagation losses of 1.47 cm^{-1} for the thin six bi-layer device. Subsequently, a set of four samples were used to characterize the modulation effect by applying square voltage pulses to the electrodes. The detector output was fed into a lock-in amplifier so that changes in the transmitted light intensity, ΔI, could be measured synchronously with the voltage pulses.

We measured the modulation depth, defined as

$$M = \frac{I_{\max} - I_{\min}}{I_{\max}} \tag{2}$$

where $I_{\max}$ and $I_{\min}$ are the maximum and minimum intensities of the transmitted signal. Figure 4 reports the dependence of M on the modulating signal amplitude at a frequency of

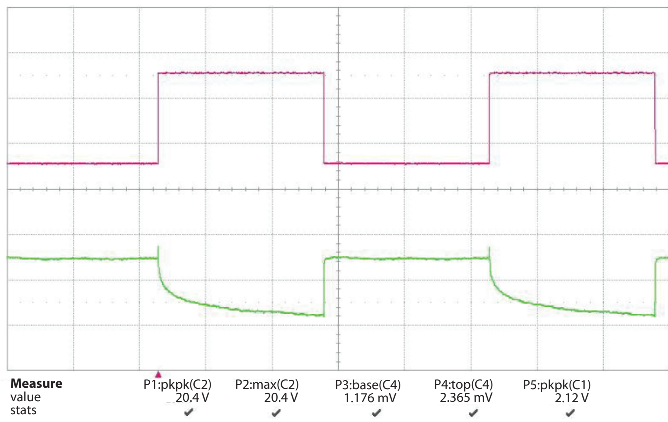

FIG. 5 Output light power and applied voltage for the thin six bi-layer 1.2 cm long waveguide. The modulating signal has $V_{\min} = 0$ V, $V_{\max} = 20$ V, duty-cycle = 50%, frequency = 10 Hz.

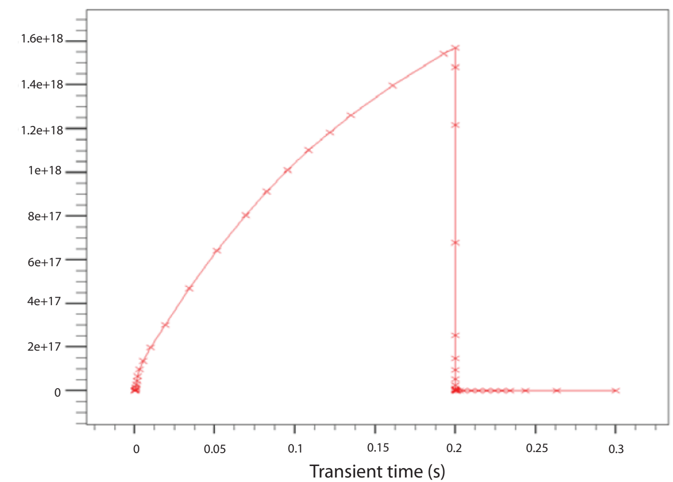

FIG. 6 Accumulated electrons/cm^{-3} at the a-silicon/dielectric interface ($x = 0.100$, $y = 0.03$ in Figure 2(a)) versus transient time for modulating signal amplitude of 30 V.

10 Hz and a duty cycle of 50%. A maximum modulation depth up to 9% is obtained for the three bi-layer sample ($L = 1.2$ cm), while a maximum modulation depth of 27% is obtained for a 1.5 cm long, thick six bi-layer, sample [12]. For the thin six bi-layer device the maximum observed modulation depth is up to 49% ($L = 1.2$ cm), measured for 20 V pulses, limited in this case by the occurrence of breakdown phenomena in the insulating layers.

The reported data show that M increases with the modulating signal amplitude and with the device length. The average effective absorption coefficient variation $\Delta\alpha_{\text{eff}}$ induced in the six bi-layer waveguide (0.5 μm-thick α-Si:H layer) is 0.11 cm^{-1}, 0.18 cm^{-1} and 0.21 cm^{-1} respectively at 10 V, 20 V and 30 V biases, corresponding to an electric field of 0.15 MV/cm, 0.30 MV/cm and 0.45 MV/cm across the 40 nm-thin insulating α-SiCN layers.

Figure 5 shows the output light power and the applied voltage as a function of time for the thin six bi-layer, 1.2 cm long, waveguide for 20 V amplitude applied pulses. We calculated a $M_{\%} = 49.6\%$.

It is evident that the device speed is mainly limited by the carrier accumulation phase following the application of the pulse. A simulation study of the carrier dynamics taking place in the α-Si:H layers reveals that the carrier accumulation is actually limited by the thermal generation and trapping phenomena, while the carrier spreading, following the bias removal, is fast, in agreement with experiments. Figure 6, for instance, shows the calculated electron count dynamics at one α-Si:H/α-SiCN interface. One way to circumvent this problem might consist in providing the α-Si:H layers with additional electrons, for example, by means of an effective doping. Figure 7 in fact summarises the results of dynamic simulations performed on the same device at different doping levels of the α-Si:H. It should be noted that the actual free carrier concentration in α-Si:H is reported in abscissa, which does not necessarily coincide with the doping level, due to carrier trapping effects by defects typical of amorphous semiconductors. From resistivity measurements we calculated that the free electron concentration in our experimental device (undoped) is close to

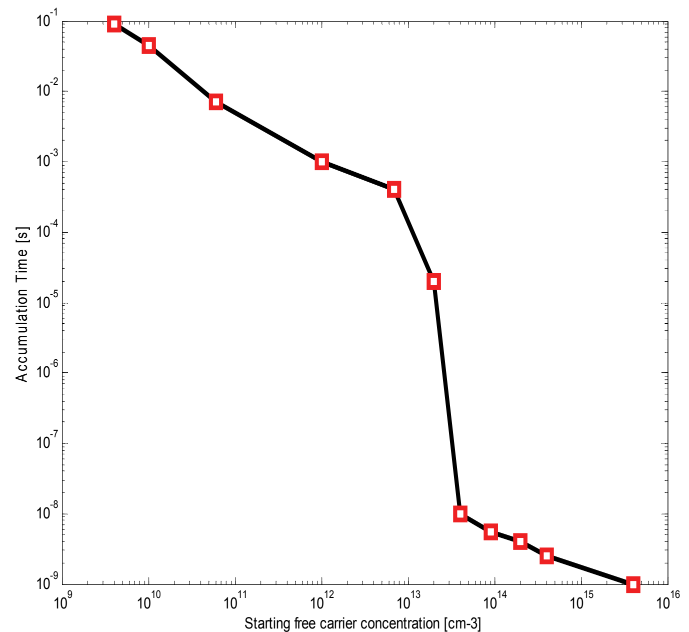

FIG. 7 Dynamic simulations versus the free carrier concentration in α-Si:H.

10^{10} cm^{-3}, which returns an accumulation speed of 5×10^{-2} s, in good agreement with the experimental results of Figure 5. A net accumulation time decrease can be estimated for a free carrier concentration exceeding 10^{13} cm^{-3}, at expenses, however, of higher free carrier absorption effects in the waveguide.

4 CONCLUSION

Three multi-stack structures, based on the CMOS-compatible technology of amorphous silicon, have been explored for enhancing electro-optical modulation effects in integrated, waveguide embedded, photonic devices.

The waveguiding structures, consisting of three (six) α-Si:H/α-SiCN stacks deposited by PECVD on a c-Si substrate, were realized and characterized. They showed propagation losses lower than 2.8 dB/cm at the wavelength of 1.55 μm.

The application of an external electric field across the structure produces carrier accumulation at the intermediate semiconductor/insulator interfaces, which is in turn responsible of an enhanced optical absorption. We measured a $\Delta\alpha_{eff}$ of 0.21 cm^{-1} when an electric field of 0.45 MV/cm is applied across each α-SiCN dielectric thin film.

We found a good agreement between the simulated and experimental data, both for static and dynamic operations.

Technologically, the fabrication process involves temperatures under 220°C, which are compatible with standard microelectronic processes and in particular suitable for the realization of a photonic layer on top of an integrated circuit.

The device speed limits has been studied by means of simulations, which have shown the impact of the α-Si:H doping on the carrier dynamics.

ACKNOWLEDGMENTS

IMM-CNR, Unit of Napoli (Italy), where the optical simulations were performed, is gratefully acknowledged.

References

[1] G. Cocorullo, F. G. Della Corte, and I. Rendina, "Amorphous silicon waveguides and light modulators for integrated photonics realized by low-temperature plasma-enhanced chemical-vapor deposition" Opt. Lett. **21**, 2002–2004 (1996).

[2] M. Okamura, and S. Suzuki, "Infrared photodetection using a-Si:H photodiode" IEEE Photonic. Tech. L. **6**, 412–414 (1994).

[3] G. Cocorullo, F. G. Della Corte, R. De Rosa, I. Rendina, A. Rubino, and E. Terzini, "Amorphous silicon-based guided-wave passive and active devices for silicon integrated optoelectronics" IEEE J. Sel. Top. Quant. **4**, 997–1001 (1998).

[4] B. Han, R. Orobtchouk, T. Benyattou, P. R. A. Binetti, S. Jeannot, J. M. Fedeli, and X. J. M. Leijtens, *Comparison of optical passive integrated devices based on three materials for optical clock distribution* (European Conference on Integrated Optics, Copenhagen, pp. 1–4, 25–27 April, 2007).

[5] F. G. Della Corte, M. Gagliardi, M. A. Nigro, and C. Summonte, "In-guide pump and probe characterization of photoinduced absorption in hydrogenated amorphous silicon thin films" J. Appl. Phys. **100**, 033104 (2006).

[6] M. Zelikson, K. Weiser, A. Chack, and J. Kanicki, "Direct determination of the quadratic electro-optic coefficient in an a-Si:H based waveguide" J. Non-Cryst. Solids **198–200**, 107–110 (1996).

[7] G. Lavareda, C. Nunes de Carvalho, E. Fortunato, A. Amaral, and A. R. Ramos, "Properties of a-Si:H TFTs using silicon carbonitride as dielectric" J. Non-Cryst. Solids **338–340**, 797–801 (2004).

[8] C. A. Barrios, "Electrooptic modulation of multisilicon-on-insulator photonic wires" J. Lightwave Technol. **24**, 2146–2155 (2006).

[9] T. S. Moss, G. J. Burrell, and B. Ellis, *Semiconductor Opto-Electronics* (Butterworth and Co., London, 1973).

[10] *RSoft Photonics CAD Layout User Guide* (Rsoft Design Group, Inc. Physical Layer Division, 200 Executive Blvd. Ossining, NY 10562).

[11] R. A. Soref, J. Schmidtchen, and K. Petermann, "Large single-mode rib waveguides in Ge-Si and Si-on-SiO_2" IEEE J. Quantum Elect. **27**, 1971–1974 (1991).

[12] F. G. Della Corte, S. Rao, M. A. Nigro, F. Suriano, and C. Summonte, "Electro-optically induced absorption in α-Si:H/α-SiCN waveguiding multistacks" Opt. Express **16**, 7540–7550 (2008).